

# Rapidly evolving faint transients from stripped-envelope electron-capture supernovae

Takashi J. Moriya<sup>1,2\*</sup> and J. J. Eldridge<sup>3†</sup>

<sup>1</sup>*Division of Theoretical Astronomy, National Astronomical Observatory of Japan, 2-21-1 Osawa, Mitaka, Tokyo 181-8588, Japan*

<sup>2</sup>*Argelander Institute for Astronomy, University of Bonn, Auf dem Hugel 71, D-53121 Bonn, Germany*

<sup>3</sup>*Department of Physics, University of Auckland, Private Bag 92019, Auckland, New Zealand*

## ABSTRACT

We investigate the expected rates and bolometric light-curve properties of stripped-envelope electron-capture supernovae (ECSNe) using stellar models from the Binary Population and Spectral Synthesis (BPASS) code. We find that 0.8 per cent ( $Z = 0.020$ ) and 1.2 per cent ( $Z = 0.004$ ) of core-collapse supernovae are stripped-envelope ECSNe. Their typical ejecta masses are estimated to be about  $0.3 M_{\odot}$  ( $Z = 0.020$ ) and  $0.6 M_{\odot}$  ( $Z = 0.004$ ). Assuming ECSN explosion properties from numerical explosion simulations, an explosion energy of  $1.5 \times 10^{50}$  erg and a  $^{56}\text{Ni}$  mass of  $2.5 \times 10^{-3} M_{\odot}$ , we find that stripped-envelope ECSNe have a typical rise time of around 7 days ( $Z = 0.020$ ) or 13 days ( $Z = 0.004$ ) and peak luminosity of around  $10^{41}$  erg s<sup>-1</sup> ( $-13.8$  mag,  $Z = 0.020$ ) or  $7 \times 10^{40}$  erg s<sup>-1</sup> ( $-13.4$  mag,  $Z = 0.004$ ). Their typical ejecta velocities are around  $7000$  km s<sup>-1</sup> ( $Z = 0.020$ ) or  $5000$  km s<sup>-1</sup> ( $Z = 0.004$ ). Thus, stripped-envelope ECSNe are observed as rapidly-evolving faint transients with relatively small velocities. SN 2008ha-like supernovae, which are the faintest kind of SN 2002cx-like (a.k.a. Type Iax) supernovae, may be related to stripped-envelope ECSNe.

**Key words:** supernovae: general – supernovae: individual: SN 2008ha – supernovae: individual: SN 2010ae – binaries: general

## 1 INTRODUCTION

Core-collapse supernovae (SNe) are mostly the result of the collapse of an iron core. Stars must be massive enough to form such cores and give rise to such an event. The minimum mass is thought to be between 8 to  $10 M_{\odot}$  (Smartt 2015). In stars below this limit nuclear burning progresses only to forming an ONeMg core. However such a core may also eventually collapse and produce a SN due to electron-capture reactions (e.g. Miyaji et al. 1980; Nomoto 1984, 1987). These events are referred to as electron-capture SNe (ECSNe). Numerical simulations of ECSNe reveal that they explode with an explosion energy of  $\sim 10^{50}$  erg and synthesize  $\sim 10^{-3} M_{\odot}$  of radioactive  $^{56}\text{Ni}$  (e.g. Kitaura, Janka, & Hillebrandt 2006).

The canonical progenitor model for an ECSN is a single star that has evolved to the super-asymptotic giant branch (super-AGB) (e.g. Eldridge & Tout 2004; Siess 2007; Eldridge, Mattila & Smartt 2007; Poelarends et al. 2008; Takahashi, Yoshida, & Umeda 2013; Jones et al. 2013; Doherty et al. 2015). A super-AGB star has a hydrogen-rich envelope with a mass of several  $M_{\odot}$  around an ONeMg core sup-

ported by electron degeneracy pressure. They are otherwise similar in structure to normal AGB stars that have a CO core. Because of the hydrogen-rich envelope an ECSN from a super-AGB star is presumed to be observed as a Type II SN (Tominaga, Blinnikov, & Nomoto 2013). However the exact observational nature of explosions of super-AGB stars is uncertain. They are expected to have high mass-loss rates in a slow stellar wind which leads to a dense circumstellar environment around the star that any SN ejecta would interact with if the star was to explode (e.g. Poelarends et al. 2008; Woosley & Heger 2015). Thus it is possible that ECSNe from super-AGB stars could show signatures of the interaction between SN ejecta and dense circumstellar media (e.g. Smith 2013; Moriya et al. 2014).

However, recent evidence has begun to show that most massive stars, that give rise to core-collapse SNe, are in fact in binary systems (Raghavan et al. 2010; Sana et al. 2012, 2013; Duchene & Kraus 2013). These studies show that maybe 50 to 70 per cent of massive stars have their evolution affected by binary interactions. For around the mass range expected for ECSNe of  $\sim 8 M_{\odot}$  the binary frequency is at least 50 per cent. It has been suggested that duplicity of a star will aid its evolution to an ECSN (Nomoto 1985; Podsiadlowski et al. 2004). ECSNe from binary systems can have profoundly different observational properties

\* takashi.moriya@nao.ac.jp

† j.eldridge@auckland.ac.nz

from those from single stars. For example, most single ECSN progenitors can retain their hydrogen-rich envelope up until the time of the collapse of their ONeMg core and thus be observed as Type II SNe. This is not necessarily true for ECSNe from binary systems as binary interactions, either Roche-lobe overflow or common envelope ejection, can remove some or all of the hydrogen-rich envelope. Therefore many binary ECSNe will occur with little or no hydrogen remaining. In addition for some the remaining helium layer can also be severely depleted by the same interactions.

In this paper, we investigate observational properties of stripped-envelope ECSNe based on binary population synthesis models from the Binary Population and Spectral Synthesis (BPASS) code<sup>1</sup> (Eldridge, Izzard & Tout 2008; Eldridge, Langer & Tout 2011; Stanway, Eldridge & Becker 2016, Eldridge et al. in prep.). We take the predicted stellar properties of ECSN progenitors from BPASS that are the result of binary evolution and investigate observational properties namely event rates and bolometric light curves (LCs) of stripped-envelope ECSNe.

We first introduce the BPASS stellar evolution models and discuss ECSN rates and stripped-envelope ECSN progenitor properties in Section 2. Then, we discuss expected stripped-envelope ECSN LC properties in Section 3. We further discuss the stripped-envelope ECSN properties and possible observational candidates in Section 4. We conclude this paper in Section 5.

## 2 PROGENITOR PROPERTIES

### 2.1 Binary population synthesis model

The stellar evolution models used in this study are from the Binary Population and Spectral Synthesis, BPASS, code. The model construction is discussed in detail in Eldridge, Izzard & Tout (2008) and Eldridge, Langer & Tout (2011). Here we use the v2.0 models which are almost identical to those in earlier versions but with an expanded number of models and a revised treatment for stellar mergers which are described in Stanway, Eldridge & Becker (2016) and Eldridge et al. (in prep.). We however present a brief summary here with the relevant details to this study.

The stellar evolution models are calculated with a modified version of the Cambridge STARS code as described in Eldridge, Izzard & Tout (2008). However the resolution of the grid used to cover the initial parameters of metallicity, initial masses and initial period has been increased so that in total there is a grid of 250,000 detailed stellar models that allow us to investigate the rich diversity of the evolution of interacting binary stars. The use of detailed models allows us to accurately follow how the stellar envelope responds to mass loss – key to determining the eventual mass and fate of the star. There are many groups that study binary evolution of massive stars and its importance for massive stars is review by Vanbeveren & Mennekens (2015).

We have recently released version 2.0 of BPASS (Stanway, Eldridge & Becker 2016, Eldridge et al. in prep.). This incorporates many refinements to the code and its outputs compared to the earlier versions, mainly in the spectral

synthesis results. The results of BPASS v2.0 have already demonstrated the improvement in agreement between observations and stellar population models that arises from the inclusion of interacting binaries (e.g. Stanway, Eldridge & Becker 2016; Wofford et al. 2016; Eldridge & Maund 2016). We use an initial-mass function based on Kroupa, Tout, & Gilmore (1993), with a power-law slope of  $-1.3$  between initial masses of  $0.1$  to  $0.5 M_{\odot}$  and a slope of  $-2.35$  from  $0.5$  to  $300 M_{\odot}$ . This is combined with an initial-mass ratio of  $q = M_2/M_1$  where we have models with  $q = 0.1$  to  $0.9$  in steps of  $0.1$ . We assume that these models are equally weighted. All secondary stars contribute to the stellar mass but we do not include a companion in the stellar mass estimate if its initial mass is less than  $0.1 M_{\odot}$ . The initial-period distribution is uniformly distributed in log of the period from  $1$  day to  $10^4$  days. There are some indications that short period systems are more numerous (Sana et al. 2012; Duchêne & Kraus 2013), but we retain the uniform distribution for simplicity. The uncertainty in period distribution is degenerate with the uncertainty in how we model Roche-lobe overflow and common-envelope evolution.

Convection is modelled using mixing-length theory and mixing is modelled simultaneously with the structure with a diffusion equation that allows us to correctly follow stable semi-convection. Convective overshooting is modelled by modifying the classical Schwarzschild criterion for instability with an overshooting parameter of  $\delta_{ov} = 0.12$ , a value derived from observations of binary systems by Schroder, Pols & Eggleton (1997) and Pols et al. (1997). The mass-loss scheme is discussed in detail in Eldridge, Izzard & Tout (2008). We use the rates of Vink, de Koter & Lamers (2001) for main-sequence OB stars, the rates of Nugis & Lamers (2000) for Wolf-Rayet stars and those of de Jager, Nieuwenhuijzen & van der Hucht (1988) for all other stars. We scale the mass-loss rates applied from those observed in the local universe, such that  $\dot{M}(Z) = \dot{M}(Z_{\odot})(Z/Z_{\odot})^{\alpha}$  and  $\alpha = 0.5$  (except in the case of OB stars where  $\alpha = 0.69$ , see Vink, de Koter & Lamers 2001). There is little consensus in the literature regarding the definition of solar metallicity. Villante et al. (2014), for example, suggest the metal fraction in the Sun is rather higher than usually assumed, while some authors (Allende Prieto, Lambert, & Asplund 2002; Asplund 2005) suggest that Solar metal abundances should be revised downwards to closer to  $Z = 0.014$  (also appropriate for massive stars within 500pc of the Sun, Nieva & Przybilla 2012). We retain  $Z_{\odot} = 0.020$  for consistency with the empirical mass-loss rates which were originally scaled from this value. In this study we also use models with a metallicity of  $Z = 0.004$  for low metallicity environments like the Small Magellanic Cloud.

Our models do not include any rotational mixing, although at low metallicities we do include an approximate implementation of quasi-chemically homogeneous evolution due to rapid rotation (Eldridge, Langer & Tout 2011; Stanway, Eldridge & Becker 2016). This does not occur in the initial mass range of the ECSN progenitors as we only include this for stars with an effective initial mass greater than  $20 M_{\odot}$ . We do not include wind-accretion in our binary models. Roche-lobe overflow is assumed to occur when the primary star filled its Roche-lobe radius and the mass-loss rate is dependent on how far it overfills the Roche-lobe as described in detail in Eldridge, Izzard & Tout (2008). If the

<sup>1</sup> <http://bpass.auckland.ac.nz>

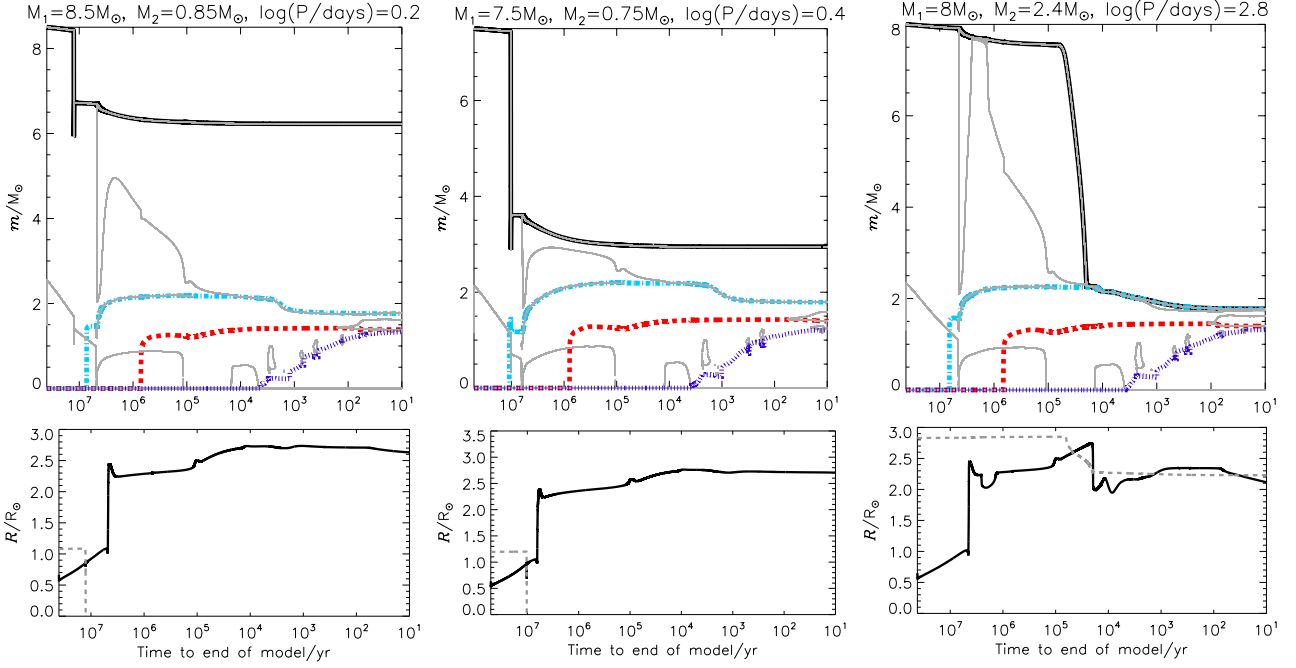


**Figure 1.** Example Kippenhahn diagrams for the evolution of ECSN progenitors. Each model is at a metallicity of  $Z = 0.020$ . The initial mass of the two stars and their initial period are given at the top of each panel. In the upper panels the solid black line shows the total mass of the star. The light-blue dash-dotted line is the edge of the helium core, the red dashed line is the edge of the CO core, the blue dotted line is the edge of the ONe core and the thin grey lines indicate convective boundaries. In the lower panels the black line indicates the radius of the primary star and the grey dashed line indicates the binary separation.

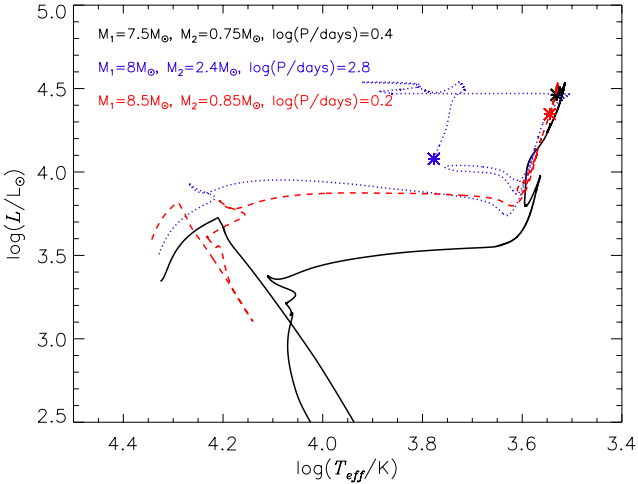


**Figure 2.** The HR diagram showing the evolution of the same models as in Figure 1.

mass loss does not prevent the star from expanding and the star grows to engulf its companion, common-envelope evolution is assumed to occur. In our code, it is numerically difficult to remove the stellar envelope instantaneously. We therefore set a high mass-loss rate and relate the decrease in the binary orbital energy to the amount of binding energy required to lose material from the surface of the primary star as described in [Eldridge, Izzard & Tout \(2008\)](#). One difference to our model now is that if the secondary star also fills its Roche-lobe during common-envelope evolution the

stars are assumed to merge and the mass of the secondary is added to the remaining mass of the primary star.

From our grid of stellar models we select out ECSN progenitors using the mass ranges of [Woosley & Heger \(2015\)](#) for the CO core mass. If a star has experienced core carbon burning and has a CO core mass between  $1.38$  and  $1.4 M_{\odot}$ , it does not experience further burning and collapses due to being above the Chandrasekhar mass. However, whether the star experiences an electron-capture SN or an iron-core collapse is uncertain and depends on how details such as the Urca process are modelled ([Jones et al. 2013](#)). We assume CO cores with masses above  $1.4 M_{\odot}$  do continue growing eventually to iron-core collapse ([Woosley & Heger 2015](#)). Stars below  $1.38 M_{\odot}$  typically require the core to grow either by helium shell burning or thermal pulses before they could collapse. We assume if this is the case that during the time for the core to grow stellar wind mass loss removes the envelope and the star forms a white-dwarf rather than an ECSN.

We note that we also require a total stellar mass greater than  $1.5 M_{\odot}$  for an ECSN to occur. Only one of our models has a massive enough CO core but is below this mass limit. Such a star below our assumed mass limit would have very small ejecta masses and correspondingly shorter timescales of their LC evolution. The LC also becomes dependent on exactly where we chose to put in a mass cut for the amount of material ejected as shown by [Tauris et al. \(2013\)](#).

We show sample evolution of some of our progenitors in Kippenhahn and Hertzsprung-Russell (HR) diagrams in Figures 1 and 2. All three example cases are at  $Z = 0.020$ . The first two cases are for stellar mergers that occur after a

short common-envelope phase during the main-sequence. In the second case the merger happens towards the end of the main-sequence and so the helium core of the star is larger than what would be expected for a similar star of the same initial mass. In the third case the common-envelope evolution occurs after core helium burning (Case C) and so their hydrogen-rich envelope is lost leaving a helium star. This star eventually becomes a helium giant which experiences another interaction reducing the helium envelope further. In all three cases we see that carbon-burning ignites centrally and burns outwards in a series of flashes. Also towards the end of the evolution we see that a convection zone opens up at the edge of the CO core. This reduces the CO core mass to below  $1.4M_{\odot}$  and prevents the ONe core from growing further. The formation of this convection zone reduces the core mass into our assumed range for ECSNe. At this point our code cannot calculate models further. The few models that we have been able to take further find that the central density increases and conditions for an ECSN can be obtained.

We stress here that while we use a detailed evolution code the ethos behind our models is to have greater accuracy in our models than using rapid stellar evolution such as that from, e.g. Hurley, Pols & Tout (2000), but we cannot calculate large numbers of detailed models over a broad initial parameter space and include all physical effects such as the models of Jones et al. (2013); Tauris, Langer & Podsiadlowski (2015) which is why we need to make assumptions about which of our models will experience ECSNe. We note that our helium star models are similar to those recently discussed by Tauris, Langer & Podsiadlowski (2015). Therefore while our evolutionary models are not evolved until the point of core collapse their similarity to these models suggests that they will do so. An advantage of our models is that we include ECSNe from both primary and secondary star as well as via mergers, by following all possible channels, allowing us to estimate the rates of these events.

The channels for the ECSNe are similar at both metallicities as shown in Figure 1. The initial mass range of the progenitors at  $Z = 0.020$  ranges from 4 to  $12 M_{\odot}$ . The two channels are either Case A mass-transfer that normally leads to a stellar merger. When mergers occur earlier in the main-sequence the final mass of the progenitor is similar to that expected from single-star ECSN evolution. Later Case A mergers tend to have less massive hydrogen-rich envelopes at the time of core-collapse. The other main channels are later Case B or Case C interactions which avoid a merger and remove the hydrogen-rich envelopes leaving helium stars as described by Podsiadlowski et al. (2004). Due to the low mass of the helium stars these tend to become helium giants and some experience a second binary interaction that reduces the helium envelope mass. The nature of the progenitors when they explode in both cases are relatively cool and luminous progenitors as those with hydrogen-rich envelopes are cooler than the helium progenitors.

## 2.2 Stripped-envelope ECSN progenitor properties

Table 1 summarizes predicted rates of ECSNe from BPASS. The total ECSN fractions in core-collapse SNe are 1.5 per cent for  $Z = 0.020$  and 8.6 per cent for  $Z = 0.004$ . This

**Table 1.** The relative fraction for ECSNe as estimated from BPASS. Statistical errors are presented.

$Z^a$	ECSN fraction <sup>b</sup>	Type distribution in ECSNe		
		Type I	Type IIb	Type II
0.020	$0.015 \pm 0.002$	$0.42 \pm 0.09$	$0.09 \pm 0.05$	$0.49 \pm 0.12$
0.004	$0.086 \pm 0.006$	$0.11 \pm 0.02$	$0.03 \pm 0.01$	$0.86 \pm 0.12$

<sup>a</sup> Initial progenitor metallicity.

<sup>b</sup> Fractions of ECSNe in core-collapse SNe.

increase is due to less mass loss because of weaker stellar wind at the lower metallicity.

We further show expected SN-type fractions of ECSNe in Table 1. We classify ECSNe from progenitors with a remaining hydrogen mass less than  $0.5 M_{\odot}$  as stripped-envelope ECSNe (Type IIb and Type I) and the others as Type II. Type IIb SNe are typically estimated to have hydrogen masses of  $0.1 - 0.5 M_{\odot}$  (e.g. Woosley et al. 1994) and we choose  $0.5 M_{\odot}$  as the dividing mass. We find in our models that few models lie close to this mass with most have a few  $M_{\odot}$  of hydrogen or no hydrogen. We find that 51 per cent of ECSN progenitors at  $Z = 0.020$  are stripped-envelope ECSNe and the fraction reduces to 14 per cent at  $Z = 0.004$ . However, the stripped-envelope ECSN fractions in core-collapse SNe are slight higher at  $Z = 0.004$  (1.2 per cent) than at  $Z = 0.020$  (0.8 per cent). This suggests that at lower metallicity there more Type II ECSNe.

We divide stripped-envelope ECSNe into two different subtypes, Type IIb and Type I. Those with hydrogen mass between  $0.5 M_{\odot}$  and  $0.01 M_{\odot}$  are classified as Type IIb and the others as Type I because even small amounts of hydrogen can be observed in SN spectra (e.g. Dessart et al. 2011; Hachinger et al. 2012). The majority of stripped-envelope ECSNe are Type I. We do not sub-classify Type I here. Whether Type I SNe are classified as Type Ib or Ic depends on the degree of  $^{56}\text{Ni}$  mixing (e.g. Dessart et al. 2012). All the Type I ECSNe we obtain have helium masses of more than  $0.06 M_{\odot}$ , which is the maximum amount of helium that can be hidden (Hachinger et al. 2012). Thus, if sufficient  $^{56}\text{Ni}$  mixing occurs, Type I ECSNe may be observed as Type Ib SNe.

Because the explosion energy ( $E_{\text{ej}}$ ) and the  $^{56}\text{Ni}$  mass ( $M_{56\text{Ni}}$ ) are expected to vary little among ECSNe, the ejecta mass ( $M_{\text{ej}}$ ) is the most influential parameter determining the LC properties of stripped-envelope ECSNe. Figure 3 shows the ejecta mass distributions of stripped-envelope ECSNe from BPASS. A typical ejecta mass of stripped-envelope ECSNe is expected to be of the order of  $0.1 M_{\odot}$ . The average ejecta mass increases as the metallicity decreases because of the scaling of stellar winds by initial metallicity as described above.

## 3 STRIPPED-ENVELOPE ECSN LIGHT CURVES

### 3.1 Method

We calculate bolometric LCs of stripped-envelope ECSNe by using a simplified analytic method introduced by Arnett (1982). This simplified method has been used to obtain

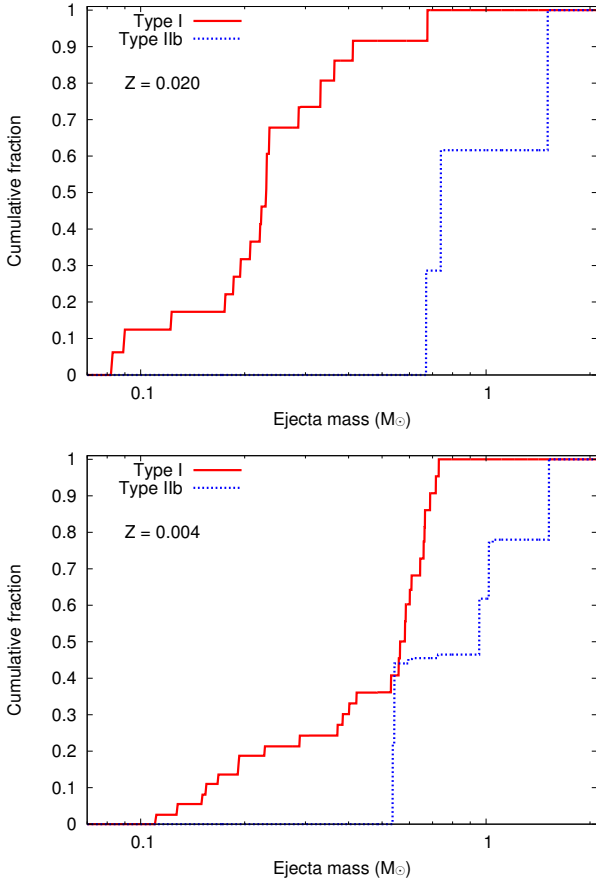


**Figure 3.** The cumulative ejecta mass distribution for the EC-SNe taken from BPASS. The upper panel is for a metallicity of  $Z = 0.020$  and the lower panel is for a metallicity of  $Z = 0.004$ .

bolometric LCs of stripped-envelope SNe where the effect of hydrogen recombination in opacity is negligible (e.g. Valenti et al. 2008; Chatzopoulos, Wheeler, & Vinko 2012; Inserra et al. 2013). Briefly, we numerically evaluate the following equation to obtain the bolometric luminosity  $L$  at time  $t$  after the explosion,

$$L(t) = \int_0^{\frac{t}{\tau_m}} 2\tau_m^{-2} D L_{\text{decay}}(t') t' e^{\left(\frac{t-t'}{\tau_m}\right)^2} dt', \quad (1)$$

where  $\tau_m$  is the effective diffusion time,  $L_{\text{decay}}(t)$  is the energy input from the nuclear decay of  $^{56}\text{Ni} \rightarrow ^{56}\text{Co} \rightarrow ^{56}\text{Fe}$ , and  $D$  is the deposition function (Arnett 1982). We only consider gamma-rays from the nuclear decay as a heating source in SN ejecta. Assuming the homogeneous density distribution,  $\tau_m$  can be expressed as

$$\tau_m = \left(\frac{6}{5}\right)^{0.25} \left(\frac{\kappa_e}{\beta c}\right)^{0.5} M_{\text{ej}}^{0.75} E_{\text{ej}}^{-0.25}, \quad (2)$$

where  $\kappa_e$  is an electron-scattering opacity in SN ejecta,  $c$  is the speed of light, and  $\beta \simeq 13.8$  (Arnett 1982). The electron-scattering opacity is assumed to be  $0.1 \text{ cm}^2 \text{ g}^{-1}$ . The deposition function  $D$  approximately takes the gamma-ray trapping efficiency in SN ejecta into account. It is evaluated as in Arnett (1982) by assuming the gamma-ray opacity of  $0.03 \text{ cm}^2 \text{ g}^{-1}$  (e.g. Colgate, Petschek, & Kriese 1980).

Both one- and two-dimensional numerical explosion

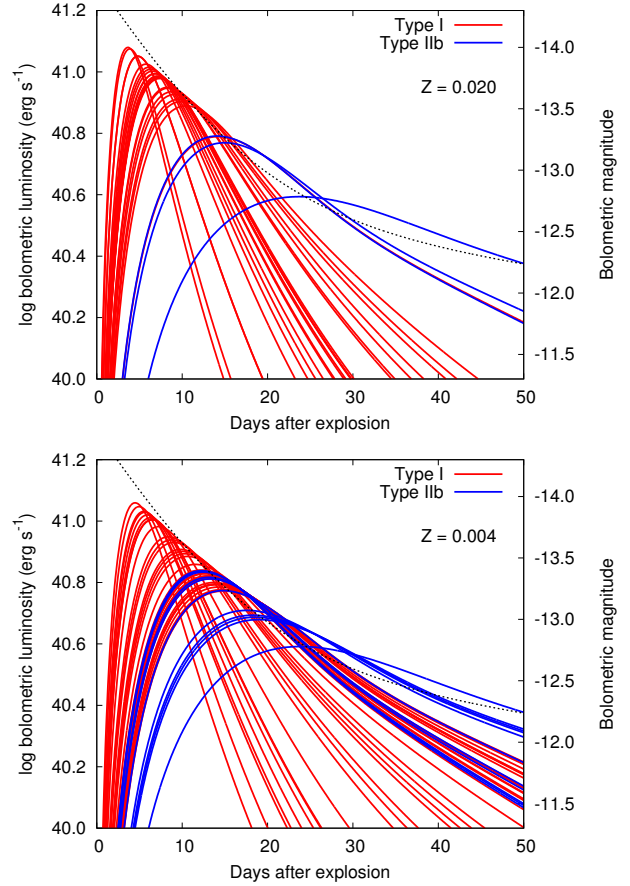


**Figure 4.** Bolometric LCs of stripped-envelope ECSNe. We show LCs of all the ECSN progenitors from BPASS and each line represents a bolometric LC from a progenitor. The dotted lines are the total available nuclear energy from  $2.5 \times 10^{-3} M_{\odot}$  of  $^{56}\text{Ni}$ . The upper panel is for a metallicity of  $Z = 0.020$  and the lower panel is for  $Z = 0.004$ .

simulations of ECSNe consistently show that their explosion energy and  $^{56}\text{Ni}$  mass are  $\sim 10^{50}$  erg and  $\sim 10^{-3} M_{\odot}$ , respectively (Kitaura, Janka, & Hillebrandt 2006; Burrows, Dessart, & Livne 2007; Wanajo et al. 2009; Wanajo, Janka, Müller 2011). Thus, the LC diversity of stripped-envelope ECSNe mostly come from the diversity in  $M_{\text{ej}}$  (Fig. 3). We take  $M_{\text{ej}}$  from the population synthesis model and fix  $E_{\text{ej}} = 1.5 \times 10^{50}$  erg and  $M_{^{56}\text{Ni}} = 2.5 \times 10^{-3} M_{\odot}$  in our LC calculations (Wanajo, Janka, Müller 2011).

### 3.2 Results

Figure 4 presents bolometric LCs of stripped-envelope EC-SNe. Each line presents a LC from a progenitor obtained from BPASS. However, the likelihood to obtain each progenitor is not taken into account in Figure 4. Figure 5 shows the expected distributions of their peak luminosity and rise time in which the probability distribution from the BPASS model is taken into account.

The typical rise time of stripped-envelope ECSN LCs is about 7 days ( $Z = 0.020$ ) and 13 days ( $Z = 0.004$ ) which are much shorter than typical stripped-envelope SNe (e.g. Drout et al. 2011; Taddia et al. 2015b; Lyman et al. 2016). The rise

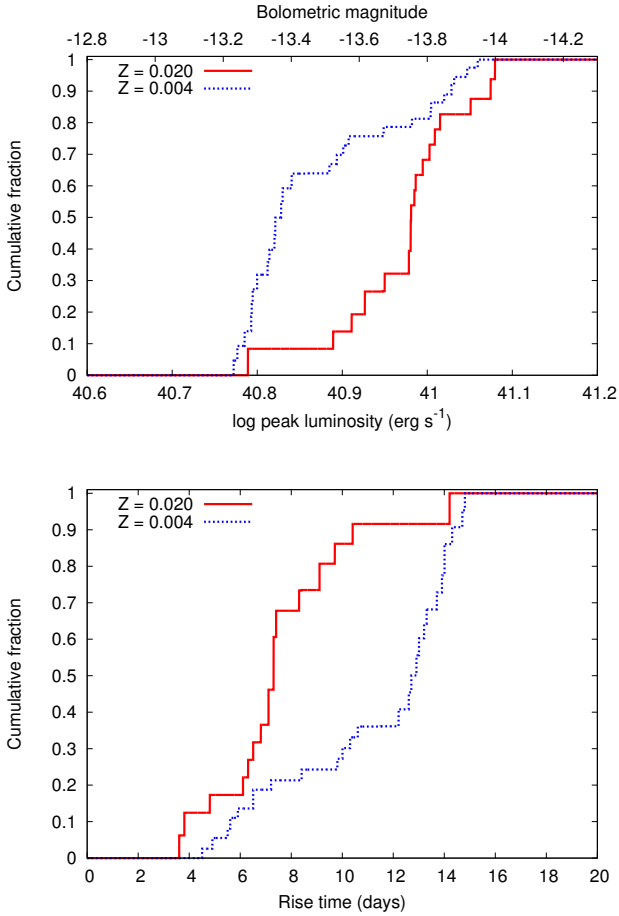


**Figure 5.** The upper panel shows the cumulative peak luminosity distribution of stripped-envelope ECSNe. The lower panel shows the cumulative rise time distributions of stripped-envelope ECSNe.

time is generally shorter in the higher metallicity models because of the smaller ejecta mass (Figure 3). The peak luminosity of stripped-envelope ECSNe is very faint because of their small  $^{56}\text{Ni}$  mass. Their typical peak luminosity is expected to be around  $10^{41} \text{ erg s}^{-1}$  ( $-13.8 \text{ mag}$ ,  $Z = 0.020$ ) or  $7 \times 10^{40} \text{ erg s}^{-1}$  ( $-13.4 \text{ mag}$ ,  $Z = 0.004$ ). After reaching the peak luminosity, the LCs decline very rapidly with a similar timescale to their rise. The luminosity does not reach the possible maximum from nuclear energy deposition because the small ECSN ejecta masses cause inefficient gamma-ray trapping and gamma-rays from the nuclear decay cannot heat the ejecta to a great amount.

There are several caveats in our simplified LC model. First, we have fixed  $E_{\text{ej}}$  in our models which can mainly affect the rise time. However, as the rise time is roughly proportional to  $\kappa_e (M_{\text{ej}}^3 / E_{\text{ej}})^{1/4}$  (Arnett 1982), a small variation in  $E_{\text{ej}}$  has little effect on the rise time compared to  $M_{\text{ej}}$ . We also fixed  $M_{56\text{Ni}}$  which mainly changes the peak luminosity. If the  $M_{56\text{Ni}}$  can vary by the factor of a few, then the LC will also vary by the same factor (about 1 mag). Even then stripped-envelope ECSNe will still be very faint transients. We have also fixed the electron-scattering opacity to  $0.1 \text{ cm}^2 \text{ g}^{-1}$ , although this is likely a good approximation (e.g. Inserra et al. 2013). The electron-scattering opacity

may vary especially in those progenitors with a relatively large hydrogen mass (blue LCs in Figure 4). Overall, although there are several uncertainties in our LC model due to its simplicity, we expect that general LC properties we estimate in this section remain unchanged even if we were to increase the complexity of our models.

## 4 DISCUSSION

The faintest kind of Type I SNe currently known are SN 2008ha-like events which have peak luminosity of around  $-14 \text{ mag}$  and rise times of around 10 days (e.g. SN 2008ha, Foley et al. 2009, 2010, 2016; Valenti et al. 2009; SN 2010ae, Stritzinger et al. 2014). SN 2008ha-like SNe are often regarded as a sub-class of SN 2002cx-like (Type Ia) SNe (Foley et al. 2013) and related to partial disruption of white dwarfs (e.g. Kromer et al. 2015). We find that bolometric LCs of stripped-envelope ECSNe are consistent with those of SN 2008ha-like SNe. Assuming typical ejecta masses of  $0.3 M_{\odot}$  ( $Z = 0.020$ ) and  $0.6 M_{\odot}$  ( $Z = 0.004$ ), we can estimate the typical ejecta velocities would be  $7000 \text{ km s}^{-1}$  ( $Z = 0.020$ ) and  $5000 \text{ km s}^{-1}$  ( $Z = 0.004$ ). The small photospheric velocities of SN 2008ha-like SNe are consistent with these estimates, particularly for the low metallicity model progenitors.

The observed SN of this group that best matches our progenitor models is SN 2010ae. The estimated explosion properties for SN 2010ae were,  $E_{\text{ej}} \sim 10^{50} \text{ erg}$ ,  $M_{\text{ej}} \sim 0.1 M_{\odot}$ , and  $M_{56\text{Ni}} \sim 10^{-3} M_{\odot}$  (Stritzinger et al. 2014). These match our lowest ejecta mass stripped-envelope ECSN models.

Spectra of SN 2008ha-like SNe are characterized by features of intermediate-mass elements (Foley et al. 2009, 2010; Stritzinger et al. 2014). In principle, spectral features from intermediate-mass elements can be observed in explosions of ONeMg cores. Enhanced production of Ca, which has been observed in SN 2008ha-like SNe, is also predicted (Wanajo, Janka, Müller 2013). Currently, spectral modelling of stripped-envelope ECSNe is lacking. We need to investigate spectral properties of stripped-envelope ECSNe and make proper comparisons with SN 2008ha-like SNe and other faint and rapid transients.

It is worth noting that while no progenitors of these events have been observed, a possible red source at the position of SN 2008ha found in a late-time image may be a companion star of an ECSN progenitor (Foley et al. 2014). A detailed comparison to stellar models such as in Eldridge & Maund (2016) is beyond the scope of this paper. We do find some of our models do transfer a large amount of mass to the companion star which would accelerate its evolution and so it could be observed as a cool red star after the explosion of the progenitor star.

Both SN 2008ha and SN 2010ae are found in low metallicity environments which are close to that of the Large Magellanic Cloud (Foley et al. 2009; Stritzinger et al. 2014). They also appear in star-forming galaxies and have short delay time (Foley et al. 2014). We find that stripped-envelope ECSN rates are higher in lower metallicity environments, and this can explain the possible preference of SN 2008ha-like SNe appearing in low metallicity environ-

ments<sup>2</sup>. Because we expect many more Type II ECSNe in lower metallicity environments (Table 1), Type II ECSNe have also likely been detected already if SN 2008ha-like SNe are stripped-envelope ECSNe. It is interesting to note that Type IIIn-P SNe which are suggested to be ECSNe (e.g. Kankare et al. 2012; Mauerhan et al. 2013) may also prefer lower metallicity environments (Taddia et al. 2015a), and they may correspond to Type II ECSNe we predict to exist.

Although SN 2002cx-like SNe share some common properties, they are also diverse (Foley et al. 2013). Most of them are likely related to explosions or eruptions of white dwarfs, but some of them, especially the faintest ones like SN 2008ha, may be related to ECSNe as we suggest here. It is also interesting to note that Jones et al. (2016) recently argue that oxygen deflagration in ONeMg cores may actually result in partial disruption of the ONeMg cores. In addition, massive stars other than ECSN progenitors can also end up with rapidly-evolving faint transients (e.g. Tauris et al. 2013; Moriya et al. 2010). Further LC and spectral modelling of stripped-envelope ECSNe are required to identify transients corresponding to stripped-envelope ECSNe.

We are not the first to connect SN 2008ha and ECSNe. Pumo et al. (2009) made this link in the context of single-star evolution model. We have shown here that stripped-envelope ECSNe can also naturally arise from binary evolution.

Finally it is also tempting to compare these LCs to the rapidly evolving transients found by Drout et al. (2014). While the timescale of the transients and our predicted rate of a few per cent is similar to those of these objects, the luminosities here (around  $-13$  mag  $- -14$  mag) are fainter than those found in this population ( $\sim -16$  mag or brighter).

## 5 CONCLUSIONS

We have shown that stripped-envelope ECSNe can be observed as rapidly-evolving faint transients. ECSNe are mostly considered to be explosions of super-AGB stars, but stripped-envelope ECSNe can occur especially from binary systems. The binary population synthesis model from the BPASS code predict that ECSN fractions in core-collapse SNe are 1.5 per cent ( $Z = 0.020$ ) and 8.6 per cent ( $Z = 0.004$ ). Among ECSNe, 51 per cent ( $Z = 0.020$ ) and 14 per cent ( $Z = 0.004$ ) are predicted to be stripped-envelope ECSNe (Table 1). Stripped-envelope ECSNe typically have ejecta masses of  $0.3 M_{\odot}$  ( $Z = 0.020$ ) and  $0.6 M_{\odot}$  ( $Z = 0.004$ ) (Figure 3).

Assuming predicted explosion properties of ECSNe ( $E_{ej} = 1.5 \times 10^{50}$  erg and  $M_{56Ni} = 2.5 \times 10^{-3} M_{\odot}$ ), we find that stripped-envelope ECSNe typically have the rise time of around 7 days ( $Z = 0.020$ ) or 13 days ( $Z = 0.004$ ) and peak luminosity of around  $10^{41}$  erg  $s^{-1}$  ( $-13.8$  mag,  $Z = 0.020$ ) or  $7 \times 10^{40}$  erg  $s^{-1}$  ( $-13.4$  mag,  $Z = 0.004$ ). The LC properties are summarized in Figures 4 and 5. Assuming the typical ejecta masses, we estimate typical ejecta velocities of  $7000$  km  $s^{-1}$  ( $Z = 0.020$ ) and  $5000$  km  $s^{-1}$  ( $Z = 0.004$ ).

Expected LC properties and ejecta velocities are consistent with those of SN 2008ha-like SNe. The stripped-envelope ECSN model can explain the preference of

SN 2008ha-like SNe to occur in low metallicity environments. The possible red source detected at the location of SN 2008ha could be a companion star of a stripped-envelope ECSN progenitor. There has not been spectral modelling of stripped-envelope ECSNe and it is required to identify them and determine if they match SN 2008ha-like SNe or other transients.

## ACKNOWLEDGEMENTS

We thank the referee for the comments improved this paper. This work is initiated during *Electron Capture Supernovae & Super-AGB Star Workshop* held at Monash University, Australia. TJM thanks Joe Lyman for comments. TJM is supported by Japan Society for the Promotion of Science Postdoctoral Fellowships for Research Abroad (26-51). JJE acknowledges support from the University of Auckland. We recognize the vital contribution of NeSI high-performance computing and the staff at the Centre for eResearch at the University of Auckland. New Zealand's national facilities are provided by the New Zealand eScience Infrastructure (NeSI) and funded jointly by NeSI's collaborator institutions and the Ministry of Business, Innovation and Employments Infrastructure programme.

## REFERENCES

- Allende Prieto C., Lambert D. L., Asplund M., 2002, ApJ, 573, L137  
 Arnett W. D., 1982, ApJ, 253, 785  
 Asplund M., 2005, ARA&A, 43, 481  
 Burrows A., Dessart L., Livne E., 2007, AIPC, 937, 370  
 Chatzopoulos E., Wheeler J. C., Vinko J., 2012, ApJ, 746, 121  
 Colgate S. A., Petschek A. G., Kriese J. T., 1980, ApJ, 237, L81  
 de Jager C., Nieuwenhuijzen H., van der Hucht K. A., 1988, A&AS, 72, 259  
 Dessart L., Hillier D. J., Livne E., Yoon S.-C., Woosley S., Waldman R., Langer N., 2011, MNRAS, 414, 2985  
 Dessart L., Hillier D. J., Li C., Woosley S., 2012, MNRAS, 424, 2139  
 Doherty C. L., Gil-Pons P., Siess L., Lattanzio J. C., Lau H. H. B., 2015, MNRAS, 446, 2599  
 Drout M. R., et al., 2011, ApJ, 741, 97  
 Drout M. R., et al., 2014, ApJ, 794, 23  
 Duchêne G., Kraus A., 2013, ARA&A, 51, 269  
 Eldridge J. J., Izzard R. G., Tout C. A., 2008, MNRAS, 384, 1109  
 Eldridge, J. J., Langer N., Tout C. A., 2011, MNRAS, 414, 3501E  
 Eldridge J. J., Mattila S., Smartt S. J., 2007, MNRAS, 376, 52  
 Eldridge, J. J., Maund J. R., MNRAS, in press (arXiv:1604.05050)  
 Eldridge J. J., Tout C. A., 2004, MNRAS, 353, 87  
 Foley R. J., Brown P. J., Rest A., Challis P. J., Kirshner R. P., Wood-Vasey W. M., 2010, ApJ, 708, L61  
 Foley R. J., Jha S. W., Pan Y.-C., Zheng W., Bildsten L., Filippenko A. V., Kasen D., 2016, arXiv, arXiv:1601.05955  
 Foley R. J., McCully C., Jha S. W., Bildsten L., Fong W.-f., Narayan G., Rest A., Stritzinger M. D., 2014, ApJ, 792, 29  
 Foley R. J., et al., 2013, ApJ, 767, 57  
 Foley R. J., et al., 2009, AJ, 138, 376  
 Hachinger S., Mazzali P. A., Taubenberger S., Hillebrandt W., Nomoto K., Sauer D. N., 2012, MNRAS, 422, 70  
 Hurley J. R., Pols O. R., Tout C. A., 2000, MNRAS, 315, 543  
 Inerra C., et al., 2013, ApJ, 770, 128  
 Jones S., Hirschi R., Nomoto K., 2014, ApJ, 797, 83J

<sup>2</sup> There are only a few SN 2008ha-like SNe found so far and this preference has not yet been confirmed statistically.

Jones S., Roepke F. K., Pakmor R., Seitenzahl I. R., Ohlmann S. T., Edelmann P. V. F., 2016, arXiv, arXiv:1602.05771

Jones S., et al., 2013, *ApJ*, 772, 150

Kankare E., et al., 2012, *MNRAS*, 424, 855

Kitaura F. S., Janka H.-T., Hillebrandt W., 2006, *A&A*, 450, 345

Kromer M., et al., 2015, *MNRAS*, 450, 3045

Kroupa P., Tout C. A., Gilmore G., 1993, *MNRAS*, 262, 545

Lyman J. D., Bersier D., James P. A., Mazzali P. A., Eldridge J. J., Fraser M., Pian E., 2016, *MNRAS*, 457, 328

Mauerhan J. C., et al., 2013, *MNRAS*, 431, 2599

Miyaji S., Nomoto K., Yokoi K., Sugimoto D., 1980, *PASJ*, 32, 303

Moriya T. J., Tominaga N., Langer N., Nomoto K., Blinnikov S. I., Sorokina E. I., 2014, *A&A*, 569, A57

Moriya T., Tominaga N., Tanaka M., Nomoto K., Sauer D. N., Mazzali P. A., Maeda K., Suzuki T., 2010, *ApJ*, 719, 1445

Nieva M.-F., Przybilla N., 2012, *A&A*, 539A, 143N

Nomoto K., 1987, *ApJ*, 322, 206

Nomoto K., 1985, in *The Crab Nebula and Related Supernova Remnants*, eds. M. C. Kafatos, & R. B. C. Henry (London: Cambridge University Press), 97

Nomoto K., 1984, *ApJ*, 277, 791

Nugis T., Lamers H. J. G. L. M., 2000, *A&A*, 360, 227

Podsiadlowski P., Langer N., Poelarends A. J. T., Rappaport S., Heger A., Pfahl E., 2004, *ApJ*, 612, 1044

Poelarends A. J. T., Herwig F., Langer N., Heger A., 2008, *ApJ*, 675, 614

Pols O. R., Tout C. A., Schroder K.-P., Eggleton P. P., Manners J., 1997, *MNRAS*, 289, 869

Pumo M. L., et al., 2009, *ApJ*, 705, L138

Raghavan D., McAlister H. A., Henry T. J., Latham D. W., Marcy G. W., Mason B. D., Gies D. R., White R. J., ten Brummelaar T. A., 2010, *ApJS*, 190, 1

Sana H., et al., 2012, *Science*, 337, 444

Sana H., et al., 2013, *A&A*, 550, 107

Schroder K.-P., Pols O. R., Eggleton P. P., 1997, *MNRAS*, 285, 696S

Siess L., 2007, *A&A*, 476, 893

Smartt S. J., 2015, *PASA*, 32, 16

Smith N., 2013, *MNRAS*, 434, 102

Stanway E. R., Eldridge J. J., Becker G. D., 2016, *MNRAS*, 456, 485

Stritzinger M. D., et al., 2014, *A&A*, 561, A146

Taddia F., et al., 2015a, *A&A*, 580, A131

Taddia F., et al., 2015b, *A&A*, 574, A60

Takahashi K., Yoshida T., Umeda H., 2013, *ApJ*, 771, 28

Tauris T. M., Langer N., Moriya T. J., Podsiadlowski P., Yoon S.-C., Blinnikov S. I., 2013, *ApJ*, 778, L23

Tauris T. M., Langer N., Podsiadlowski P., 2015, *MNRAS*, 41, 2123

Tominaga N., Blinnikov S. I., Nomoto K., 2013, *ApJ*, 771, L12

Valenti S., et al., 2009, *Nature*, 459, 674

Valenti S., et al., 2008, *MNRAS*, 383, 1485

Vanbeveren D., Mennekens N., 2015, arXiv: 1508.04282

Villante F. L., Serenelli A. M., Delahaye F., Pinsonneault M. H., 2014, *ApJ*, 787, 13

Vink J. S., de Koter A., Lamers H. J. G. L. M., 2001, *A&A*, 369, 574

Wanajo S., Janka H.-T., Müller B., 2013, *ApJ*, 767, L26

Wanajo S., Janka H.-T., Müller B., 2011, *ApJ*, 726, L15

Wanajo S., Nomoto K., Janka H.-T., Kitaura F. S., Müller B., 2009, *ApJ*, 695, 208

Wofford A., et al., 2016, arXiv, arXiv:1601.03850

Woosley S. E., Eastman R. G., Weaver T. A., Pinto P. A., 1994, *ApJ*, 429, 300

Woosley S. E., Heger A., 2015, *ApJ*, 810, 34

This paper has been typeset from a  $\text{\TeX}/\text{\LaTeX}$  file prepared by the author.